Heterogeneity in the Binding of Lipid Molecules to the Surface of a Membrane Protein: Hot Spots for Anionic Lipids on the Mechanosensitive Channel of Large Conductance MscL and Effects on Conformation†

Andrew M. Powl, J. Malcolm East, and Anthony G. Lee*

School of Biological Sciences, University of Southampton, Southampton SO16 7PX, U.K.

Received December 7, 2004; Revised Manuscript Received February 17, 2005

ABSTRACT: We have introduced single Trp residues into the mechanosensitive channel of large conductance (MscL) from *Mycobacterium tuberculosis* and used fluorescence quenching by brominated phospholipids to detect the presence of a binding site of high affinity for anionic phospholipids. A cluster of three positively charged residues, Arg-98, Lys-99, and Lys-100, is located on the cytoplasmic side of MscL, in a position where they could interact with the headgroup of an anionic phospholipid. Single mutations of these charged residues in the Trp-containing mutant F80W results in a decreased affinity for phosphatidic acid. Single mutations of the charged residues also result in a significant shift in the fluorescence emission spectrum in dioleoylphosphatidylcholine [di(C18:1)PC] but smaller shifts in dioleoylphosphatidic acid [di(C18:1)PA], suggesting that single mutations result in a conformational change for the protein that is reversed by interaction with anionic phospholipids. This is consistent with the observation that single mutations of the charged residues do not result in a gain of function phenotype. In contrast, simultaneous mutation of all three charged residues results in a gain of function phenotype, and a shift in fluorescence emission spectrum in di(C18:1)PC not reversed in di(C18:1)PA. The gain of function mutant F80W:V21K also shows a shifted fluorescence emission spectrum in both di(C18:1)PC and di(C18:1)PA and binds di(C18:1)PC and di(C18:1)PA with equal affinity, suggesting that the conformational change caused by the V21K mutation results in a breakup of the cluster of three positive charges. Experiments with the Trp mutants L69W and Y87W allow us to measure lipid binding constants on the periplasmic and cytoplasmic sides of the membrane, respectively. On both sides of the membrane the affinity for di(C18:1)PC is equal to that for dioleoylphosphatidylethanolamine. On the periplasmic side of the membrane, there is no selectivity for anionic phospholipids. In contrast, quenching data for Y87W provides evidence for the existence of two lipid binding sites on the cytoplasmic side of the membrane close to the Trp residue at position 87, with binding to one of these sites showing a marked preference for anionic lipid over zwitterionic lipid, presumably involving the charged cluster Arg-98, Lys-99, and Lys-100.

The hydrophobic surface of an intrinsic membrane protein is heterogeneous and rough. In a membrane, this surface will be covered by a shell of lipid molecules, referred to as boundary or annular lipids, these lipid molecules acting as a "solvent" for the protein (*1*). The basic properties of these lipid molecules have been defined by electron spin resonance (ESR) and fluorescence experiments. ESR studies show that the rotational mobility of the annular lipids is impeded by interaction with the protein and that the lipid fatty acyl chains are not as well oriented as those of the bulk lipids (*2*). ESR studies also show that the annular lipid molecules are in fast exchange with bulk lipid molecules; the off rate for a phosphatidylcholine for example is about $(1-2) \times 10^7$ s^{-1} at 30 °C, only slightly slower than the rate of exchange of two lipid molecules in the bulk phase (ca. 8×10^7 s^{-1} at 30 °C) (*2*−*4*). This relatively fast off-rate suggests that the lipid−protein interaction is a relatively nonsticky one, showing little selectivity. Indeed, direct measurements of lipid binding constants using ESR and fluorescence methods show that most lipid molecules do bind to the surfaces of membrane proteins with little selectivity (*1*, *2*, *5*, *6*). However, there is also strong evidence for the existence of more specific binding of small numbers of lipid molecules to some membrane proteins. Some of these lipid molecules bind between transmembrane α-helices, often at protein−protein interfaces in multimeric membrane proteins, and most of the lipid molecules identified in X-ray crystal structures of membrane proteins correspond to lipid molecules of this type (*1*, *7*). Nevertheless, X-ray crystal structures of some membrane proteins, including bacteriorhodopsin (*8*), succinate dehydrogenase from *Escherichia coli* (*9*), and the ADP/ATP carrier from mitochondria (*10*), show resolved lipid molecules bound to the surface of the protein, not buried within deep clefts (*11*). Although bacteriorhodopsin may represent a special case, bacteriorhodopsin being located in quasi-crystalline membrane patches in the membranes of *Halobacterium salinarum*, the other examples suggest that the lipid-bound surface of a membrane protein could be heterogeneous, with some lipid molecules binding more

† We thank the BBSRC for a studentship (to A.M.P.).

* To whom correspondence should be addressed. Phone: 44 (0) 2380 594331. Fax: 44 (0) 2380 594459. E-mail: agl@soton.ac.uk.

10.1021/bi047439e CCC: $30.25
Published on Web 03/25/2005

tightly than others. In particular, the presence of a cluster of positively charged residues on the surface of a membrane protein close to the lipid−water interface could produce a "hot spot" for binding an anionic lipid molecule, the anionic lipid molecule being attracted to this region by nonspecific, charge−charge interactions.

Since existing ESR and fluorescence techniques report on the average properties of the bound lipid molecules, establishing the presence of heterogeneous lipid binding requires a new approach. Here we show that quenching of Trp fluorescence by bromine-containing phospholipids has the spatial resolution required to resolve distinct patterns of lipid binding on the surface of a membrane protein. Bromine-containing phospholipids are made by addition of bromine across the double bonds of phospholipids containing two oleyl chains: these lipids behave much like a conventional phospholipid with unsaturated fatty acyl chains, because the bulky bromine atoms have effects on lipid packing that are similar to those of a cis double bond (*12*). The efficiency of quenching of Trp fluorescence by phospholipids containing dibrominated fatty acyl chains depends on the sixth power of the distance between the Trp and the dibromo group with a value for R_o, the distance at which energy transfer is 50% efficient, of 8 Å (*5*, *13*). The short range of the quenching process means that only binding events in the immediate vicinity of a Trp residue can affect its fluorescence. If a membrane protein containing a single Trp residue is reconstituted into bilayers containing a mixture of brominated and nonbrominated phospholipids, the degree of quenching of the tryptophan fluorescence will depend on the fraction of the phospholipid molecules bound next to the Trp residue that are brominated and thus on the strength of binding of the brominated phospholipid at sites close to the Trp residue. If the Trp residue is located on the cytoplasmic side of the membrane, fluorescence quenching experiments will give relative lipid binding constants in the cytoplasmic leaflet of the lipid bilayer, and, similarly, a Trp residue on the external side of the membrane will give relative lipid binding constants in the external leaflet of the lipid bilayer. Further, if the Trp residue is located close to a cluster of positively charged residues making up a hot spot for binding anionic lipids on the protein, then fluorescence quenching experiments would show stronger binding of anionic lipids than zwitterionic lipids in the vicinity of the Trp residue; mutation of the charged residues making up the hot spot would be expected to decrease the measured affinity for anionic lipids compared to zwitterionic lipids.

We have tested these ideas using the mechanosensitive channel of large conductance MscL. The crystal structure of MscL from *Mycobacterium tuberculosis* (*14*) shows the channel to be a homopentamer, each monomer containing two transmembrane α-helices, the second of which (TM2) is lipid-exposed (Figure 1). The protein has the advantage for the proposed experiments that it contains no Trp residues. MscL opens on increasing tension in a membrane, and, because MscL is fully functional when reconstituted alone into lipid vesicles, membrane tension must be transduced directly from the lipid molecules to the protein (*15*, *16*). Interaction between the lipid bilayer and the protein is therefore particularly important for MscL.

The crystal structure of MscL shown in Figure 1 corresponds to the closed form of the channel. On increasing the tension in the membrane, MscL passes through a series of at least five subconducting states before reaching the open state in which the diameter of the pore has increased from ca. 2 Å to ca. 30−40 Å (*15*). Random and site directed mutagenesis of MscL have identified two phenotypes, gain of function mutants that result in the channel opening either spontaneously or at very low tensions, and loss of function mutants where opening is either abolished completely or requires higher tension than for the wild-type protein (*17*). Gain of function mutants can be detected by a reduced rate of growth of bacteria expressing the mutant, due to an inability to retain osmoprotectants and maintain turgor pressure (*18*). Severe loss of function mutants can be detected by loss of the ability to rescue *E. coli* strains lacking mechanosensitive channels from lysis on transferring to a medium of low osmotic strength (*5*, *17*, *19*). Gain of function mutants of *E. coli* MscL have been generated by mutation of Gly-22 and Val-23, in the narrowest region of the pore, to a charged residue such as Lys, resulting in a channel that opens at very low or zero tension and frequently occupies a subconductance state (*18*).

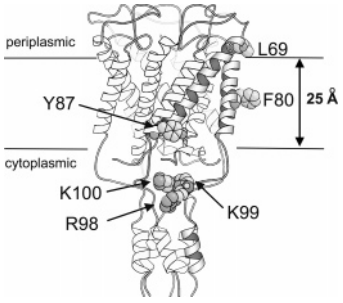

FIGURE 1: The structure of the MscL pentamer. Shown in space fill format are the residues Leu-69, Phe-80, and Tyr-87 mutated to Trp residues, and the charge residues Arg-98, Lys-99, and Lys-100. The side chain of Lys-100 is not resolved in the crystal structure and has been modeled in for illustrative purposes. The horizontal lines represent the probable location of the hydrocarbon core of the surrounding lipid bilayer (*31*). The figure was prepared using Bobscript (*30*) and the coordinates in PDB 1MSL.

In previous studies we mutated Phe-80, in the middle of the second transmembrane α-helix of MscL, to Trp (Figure 1) and determined binding constants for phospholipids to MscL from measurements of the level of Trp fluorescence quenching caused by brominated phospholipids (*5*). When there is a single class of lipid binding site on a membrane protein, binding constants determined from quenching studies in mixtures of lipid A with brominated lipid B should be the same as those determined using mixtures of brominated lipid A and nonbrominated lipid B. Although this was found to be the case for MscL in mixtures of phosphatidylcholine and phosphatidylethanolamine, it was not the case with mixtures of phosphatidylcholine with phosphatidic acid (*5*). It was therefore suggested that there are at least two classes of binding site for phosphatidic acid on MscL, one class of site showing a higher affinity for phosphatidic acid than the other (*5*). The structure of MscL shows no clear cluster of cationic residues on the periplasmic side of the membrane that might make a strong binding site for the phosphatidic acid headgroup, but a cluster of three charged residues (Arg-98, Lys-99, Lys-100) in each monomer on the cytoplasmic side of the membrane could constitute a hot spot for binding anionic lipid on the cytoplasmic side of the membrane

(Figure 1). Here we provide evidence that this cluster of charged residues does indeed constitute a hot spot for binding anionic lipid. We investigate the effects of mutating these charged residues and show, unexpectedly, that the mutations can lead to a change in conformation of MscL to an open-like state similar to that generated by introduction of a charged residue into the narrow region of the pore. Further, we show that this conformational change is reversed by the presence of anionic lipid, showing the importance of the lipid−protein interactions in determining the conformation of MscL in the membrane.

MATERIALS AND METHODS

Materials and General Procedures. Dioleoylphosphatidylcholine [di(C18:1)PC],[1] dioleoylphosphatidylethanolamine [di(C18:1)PE], dioleoylphosphatidic acid [di(C18:1)PA], dioleoylphosphatidylserine [di(C18:1)PS], and tetraoleoylcardiolipin [tetra(C18:1)CL] were obtained from Avanti Polar Lipids. The phospholipids were brominated as described in East and Lee (*12*) to give the corresponding brominated analogues, as follows: di(9,10-dibromostearoyl)phosphatidylcholine [di(Br_2C18:0)PC], di(9,10-dibromostearoyl)phosphatidylethanolamine [di(Br_2C18:0)PE], di(9,10-dibromostearoyl)phosphatidic acid [di(Br_2C18:0)PA], di(9,10-dibromostearoyl)phosphatidylserine [di(Br_2C18:0)PS], and tetra-(9,10-dibromostearoyl)cardiolipin [tetra(Br_2C18:0)CL]. The purity of the lipids was confirmed as in East and Lee (*12*).

Mutagenesis, Purification, and Reconstitution of MscL. A plasmid containing the *M. tuberculosis mscL* gene with a poly-His epitope at the N-terminus was the generous gift of Professor D. C. Rees. Site directed mutagenesis was performed using the Quick-change protocol from Stratagene. Following PCR mutagenesis the native methylated DNA templates were digested with DpnI (Promega) for 2 h at 37 °C. The mutations were confirmed by DNA sequencing.

E. coli BL21(λDE3)pLysS transformants carrying the pET-19b plasmid (Novagen) with the *mscL* gene were generally grown in 6 L Luria broth to mid-log phase ($OD_{600} = 0.6$) and then induced for 3 h in the presence of isopropyl-β-D-thiogalactopyranoside (IPTG; 1.0 mM). Gain of function mutants were grown on a larger scale, typically 60 L Luria broth, to late log phase ($OD_{600} = 1.1$) and then induced for 80 min before harvesting. MscL was purified as described by Powl et al. (*5*) and stored at −80 °C until use.

Purified MscL was reconstituted into lipid bilayers by mixing lipid and MscL in cholate at a 100:1 molar ratio of lipid to MscL monomer, followed by dilution into buffer to decrease the concentration of cholate below its critical micelle concentration, as described (*5*).

In Vivo Assays for Loss and Gain of Function Mutants. The method described in Powl et al. (*5*) was used to test for loss of function mutants. *E. coli* MJF465 transformants (*20*) carrying the pET-19b plasmid with the *mscL* gene were grown in 10 mL of LB medium containing ampicillin (100 μg mL^{-1}) and chloramphenicol (25 μg mL^{-1}) supplemented with 0.4 M NaCl for 16 h at 37 °C. The cultures (200 μL) were used to seed fresh cultures (10 mL) that were grown in the presence of IPTG for 4 h. Cells were harvested by centrifugation, and the cell pellet was resuspended in sterile 0.4 M NaCl containing ethidium bromide (0.5 μg mL^{-1}) to an apparent absorbance at 600 nm of 5. Samples of the cell suspension (30 μL) were diluted 60-fold into either 0.4 M NaCl or water, both containing ethidium bromide (0.5 μg mL^{-1}), and incubated for 45 min at room temperature followed by centrifugation at 8000*g* for 10 min. The supernatant was assayed for the release of DNA by measuring fluorescence intensities at 632 nm. Results were corrected for background light scatter by subtracting the emission of a suitable blank.

Gain of function mutants were detected by a reduced rate of growth after induction of MscL production with IPTG. *E. coli* BL21(DE3)pLysS transformants carrying the pET-19b plasmid with the *mscL* gene were grown in 10 mL of LB medium containing ampicillin (100 μg mL^{-1}) and chloramphenicol (25 μg mL^{-1}) for 16 h at 37 °C in an orbital shaker. Overnight cultures (1 mL) were used to seed fresh cultures (50 mL), which were grown at 37 °C. Cultures were induced with 1 mM IPTG upon reaching an absorbance at 600 nm of 0.2. Following induction, absorbance readings were recorded every 30 min at 600 nm.

Fluorescence Measurements and Analysis. Trp fluorescence intensities were measured at 325 nm with excitation at 280 nm, for 0.98 μM MscL in buffer (20 mM Hepes, 200 mM KCl, 1 mM EGTA, pH 7.2) at 25 °C, using an SLM 8100 fluorimeter. Intensities were corrected for light scatter by subtraction of a blank consisting of lipid alone in buffer.

Quenching of Trp fluorescence by brominated phospholipid in a mixture of a brominated phospholipid with the equivalent nonbrominated phospholipid was fitted to a lattice model for quenching (*21*, *22*) using the equation

$$F = F_{min} + (F_0 - F_{min})(1 - x_{Br})^n \quad (1)$$

Here F_0 and F_{min} are the fluorescence intensities for MscL in nonbrominated and in brominated lipid, respectively, F is the fluorescence intensity in the phospholipid mixture when the mole fraction of brominated lipid is x_{Br}, and n is the number of lipid binding sites on MscL from which the fluorescence of the Trp residue can be quenched. In a mixture of a nonbrominated lipid A and a brominated lipid B, an equilibrium will be established at each lattice site:

$$PA + B \leftrightarrows PB + A$$

where PA and PB are protein bound to lipids A and B, respectively, and the binding constant for B relative to A is given by

$$K = ([PB][A])/([PA][B]) \quad (2)$$

Fluorescence quenching in the mixture is described by the equation

$$F = F_{min} + (F_0 - F_{min})(1 - f_{Br})^n \quad (3)$$

[1] Abbreviations: di(C18:1)PC, dioleoylphosphatidylcholine; di(C18:1)PE, dioleoylphosphatidylethanolamine; di(C18:1)PA, dioleoylphosphatidic acid; di(C18:1)PS, dioleoylphosphatidylserine; tetra(C18:1)CL, tetraoleoylcardiolipin; di(Br_2C18:0)PC, di(9,10-dibromostearoyl)phosphatidylcholine; di(Br_2C18:0)PE, di(9,10-dibromostearoyl)phosphatidylethanolamine; di(Br_2C18:0)PA, di(9,10-dibromostearoyl)phosphatidic acid; di(Br_2C18:0)PS, di(9,10-dibromostearoyl)phosphatidylserine; tetra(Br_2C18:0)CL, tetra(9,10-dibromostearoyl)cardiolipin; MscL, mechanosensitive channel of large conductance; IPTG, isopropyl-β-D-thiogalactopyranoside.

where f_{Br}, the fraction of sites on MscL occupied by brominated lipid, is given by

$$f_{Br} = Kx_{Br}/(Kx_{Br} + [1 - x_{Br}]) \quad (4)$$

In a case where Trp fluorescence is quenched equally from two sites with different relative affinities for brominated lipid, quenching can be expressed as

$$F = F_{min} + (F_0 - F_{min})(1 - f^1_{Br})(1 - f^2_{Br}) \quad (5)$$

where

$$f^1_{Br} = K_1 x_{Br}/(K_1 x_{Br} + [1 - x_{Br}]) \quad (6)$$

and

$$f^2_{Br} = K_2 x_{Br}/(K_2 x_{Br} + [1 - x_{Br}]) \quad (7)$$

where K^1 and K^2 are the relative binding constants for the brominated lipid at the two sites.

Equations 1 and 3 were fitted to the experimental data using the nonlinear least-squares routine in the SigmaPlot package. An iterative procedure was used to fit the data for a set of experiments (A with brominated B and B with brominated A) to eq 5.

RESULTS

Phenotypic Properties of Charge Mutants of F80W. The three residues Arg-98, Lys-99, and Lys-100 in each monomer of MscL form a cluster on the cytoplasmic side of the membrane in a position where they could interact strongly with an anionic lipid headgroup (Figure 1). These three residues were mutated individually in F80W to Gln, and double and triple mutants were also prepared. The charge mutants of MscL were all functional in an assay for loss of function mutants, based on the ability to rescue *E. coli* strain MJF465 lacking mechanosensitive channels from the effects of osmotic downshock (data not shown). Gain of function mutants of MscL expressed in *E. coli* result in a reduced rate of growth because of an inability to retain osmoprotectants and to maintain turgor pressure (*18*). *E. coli* expressing single charge mutants of MscL and the double charge mutant F80W:K99Q:K100Q have growth curves very similar to that of *E. coli* expressing wild-type MscL (Figure 2), suggesting that these mutations do not result in a gain of function phenotype. However, *E. coli* expressing the double charge mutants F80W:R98Q:K99Q and F80W:R98Q:K100Q and the triple charge mutant F80W:R98Q:K99Q:K100Q show a marked reduction in the rate of growth (Figure 2). The growth curve for the triple charge mutant is compared in Figure 2 with that for the mutant F80W:V21K; Val-21 in MscL of *M. tuberculosis* is equivalent to Gly-22 in MscL of *E. coli*, and introduction of a charged residue into position 22 in *E. coli* MscL results in a gain of function mutant, the channel opening at lower than normal membrane tensions and resulting in a much reduced rate of cell growth (*18*). Thus the triple charge mutant F80W:R98Q:K99Q:K100Q and the two double charge mutants F80W:R98Q:K99Q and F80W:R98Q:K100Q of *M. tuberculosis* MscL show the classical gain of function phenotype, suggesting that they open at lower than normal membrane tensions.

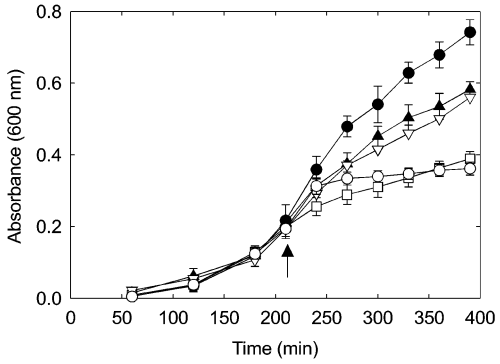

FIGURE 2: Growth of *E. coli* in liquid media expressing mutant *mscL* genes. *E. coli* BL21(DE3)pLysS transformants carrying the pET-19b plasmid with the *mscL* gene were grown at 37 °C: (●) WT, (□) F80W:V21K, (▲) F80W:R98Q, (▽) F80W:K99Q:K100Q, and (○) F80W:R98Q:K99Q:K100Q. Cells were induced with 1 mM IPTG at an absorbance at 600 nm of ca. 0.2 (arrow). Data points are the average of five colonies. Growth curves for F80W:K99Q and F80W:K100Q were very similar to that shown for F80W:R98Q, and growth curves for F80W:R98Q:K99Q and F80W:R98Q:K100Q were very similar to that shown for F80W:R98Q:K99Q:K100Q.

Fluorescence Properties of Charge Mutants of F80W. Trp fluorescence emission spectra were recorded for the charge mutants reconstituted into bilayers of di(C18:1)PC, using the environmental sensitivity of Trp fluorescence emission to look for possible changes in conformation. The fluorescence emission maximum for F80W reconstituted into bilayer of di(C18:1)PC is 321 nm, characteristic of a very hydrophobic environment for the Trp residue (Table 1). In contrast, the fluorescence emission maximum for F80W:V21K is shifted ca. 11 nm to longer wavelength, suggesting that the gain of function phenotype is associated with a major change in conformation affecting the location of the Trp residue introduced at position 80. Mutation of Arg-98, Lys-99, or Lys-100 in F80W resulted in 5−8 nm increases in fluorescence emission maxima (Table 1), suggesting that these single charge mutations also result in significant structural changes in the channel, even though the growth studies shown in Figure 2 suggest that the mutations do not result in a gain of function phenotype.

Whereas the fluorescence emission maximum for F80W is the same in di(C18:1)PC and di(C18:1)PA, the fluorescence emission maximum for F80W:V21K is slightly lower in di(C18:1)PA than in di(C18:1)PC, and for F80W:R98Q, F80W:K99Q, and F80W:K100Q fluorescence emission maxima are considerably lower in di(C18:1)PA or di(C18:1)PS than in di(C18:1)PC (Table 1), suggesting that the change in structure induced by the charge mutation is partly reversed in the presence of anionic phospholipid. Simultaneous mutation of all three residues Arg-98, Lys-99, and Lys-100 results in an 11 nm increase in fluorescence emission maximum, to a value very similar to that in F80W:V21K, consistent with the triple mutation resulting in a gain of function phenotype (Figure 2).

Fluorescence Quenching of Charge Mutants of F80W. F80W and its charge mutants were reconstituted into mixtures of lipids with two oleoyl chains and the corresponding lipid with two dibrominated fatty acyl chains. The level of fluorescence quenching in these mixtures increased with increasing content of the brominated lipid and, as shown in Figure 3 for F80W:R98Q:K99Q:K100Q, fluorescence quenching fitted to eq 1 with the values for *n*, the number

Table 1: Fluorescence Properties of Charge Mutants of MscL[a]

	phospholipid					
	di(C18:)PC		di(C18:1)PS		di(C18:1)PA	
mutant	λ^{max} (nm)	ω (nm)	λ^{max} (nm)	ω (nm)	λ^{max} (nm)	ω (nm)
F80W	321.0 ± 0.1	45.9 ± 0.2	321.1 ± 0.1	40.8 ± 0.2	320.9 ± 0.1	43.2 ± 0.2
F80W:R98Q	328.5 ± 0.1	52.6 ± 0.1	326.0 ± 0.1	54.1 ± 0.2	324.2 ± 0.1	55.4 ± 0.3
F80W:K99Q	326.9 ± 0.1	49.4 ± 0.2	323.7 ± 0.1	52.2 ± 0.2	323.9 ± 0.1	54.0 ± 0.3
F80W:K100Q	325.7 ± 0.2	46.4 ± 0.2	323.8 ± 0.1	49.5 ± 0.2	321.6 ± 0.1	49.2 ± 0.3
F80W:R98Q:K99Q:K100Q	332.4 ± 0.1	58.2 ± 0.2				
F80W:V21K	331.8 ± 0.2	51.6 ± 0.3			329.9 ± 0.2	50.4 ± 0.2

[a] Mutants of MscL were reconstituted into bilayers of the given phospholipid, and values of λ^{max}, the wavelength of maximum emission, and ω, the peak width at half-height, were determined by fitting the fluorescence emission spectra to the equation for a skewed Gaussian (*29*).

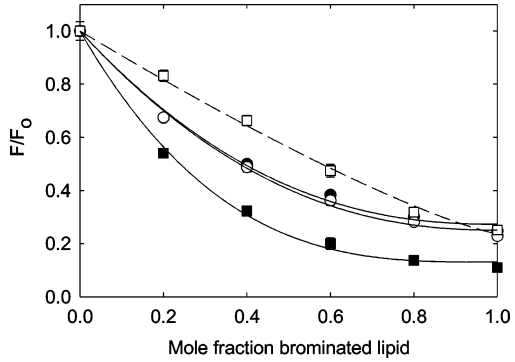

FIGURE 3: Quenching of Trp fluorescence of a charge mutant of F80W by brominated phospholipids. F80W:R98Q:K99Q:K100Q was reconstituted into bilayers containing mixtures of nonbrominated lipid and the corresponding brominated lipid. Fluorescence intensities are expressed as a fraction of the fluorescence for MscL reconstituted in mixtures of nonbrominated lipid. Lipid headgroups were as follows: (●) di(C18:1)PC, (○) di(C18:1)PS, (■) di(C18:1)PA, and (□) tetra(C18:1)CL. Data points are the average of three determinations. The lines show fits to eq 1 giving the values for *n* listed in Table 2.

of sites from which the fluorescence of the Trp residue can be quenched, given in Table 2. Values of *n* are very similar for all the lipids and all the mutants except for tetra(Br_2-C18:0)CL for which the value of *n* is about half that for the other phospholipids, consistent with the four-chain structure of cardiolipin compared to the two-chain structure of the other phospholipids. The level of quenching observed with anionic phospholipids is slightly greater than that observed with zwitterionic lipids, particularly for phosphatidic acid (Table 2), an effect observed with other membrane proteins and possibly related to the observed quenching of Trp fluorescence by acidic groups (*6*). Levels of fluorescence quenching in brominated phospholipids for the charge mutants of F80W are slightly less than for F80W itself, consistent with a conformational change on mutation of the charged residues.

Effects of mutating Arg-98, Lys-99, or Lys-100 on the binding of anionic lipids to MscL were determined in experiments studying Trp fluorescence quenching of MscL reconstituted into mixtures of di(Br_2C18:0)PC with an anionic lipid and reconstituted into mixtures of di(C18:1)-PC with a brominated anionic lipid. If there are two or more classes of binding site on MscL, each with a different affinity for anionic lipids, and if these sites are close enough to the Trp residue so that binding of a brominated lipid to these sites will cause quenching, then the binding constant obtained from the two sets of experiments will be different; binding of brominated anionic lipid to the site with highest affinity for anionic lipid will dominate quenching in the experiments with brominated anionic lipid, and binding of di(Br_2C18:0)-PC to the site with lower affinity for anionic lipid will be more important in the experiments in which the brominated lipid is di(Br_2C18:0)PC.

As previously reported (*5*), fluorescence quenching of F80W in mixtures containing phosphatidic acid fits to eq 3 but with a relative binding constant obtained from experiments with di(Br_2C18:0)PA greater than that obtained from experiments with di(Br_2C18:0)PC (Table 3), consistent with the presence of at least two classes of binding site on MscL from which the fluorescence of Trp-80 can be quenched,

Table 2: Fluorescence Quenching of Charge Mutants of F80W in Brominated Phospholipids as a Function of Lipid Headgroup[a]

phospholipid	F/F_0	n^b
	F80W	
di(Br_2C18:0)PC	0.19 ± 0.01	2.54 ± 0.05
di(Br_2C18:0)PS	0.12 ± 0.01	2.95 ± 0.22
di(Br_2C18:0)PA	0.11 ± 0.01	3.62 ± 0.27
tetra(Br_2C18:0)CL	0.09 ± 0.01	1.25 ± 0.02
	F80W:R98Q	
di(Br_2C18:0)PC	0.37 ± 0.02	2.40 ± 0.22
di(Br_2C18:0)PS	0.28 ± 0.02	2.39 ± 0.19
di(Br_2C18:0)PA	0.25 ± 0.02	2.41 ± 0.17
tetra(Br_2C18:0)CL	0.25 ± 0.02	1.14 ± 0.08
	F80W:K99Q	
di(Br_2C18:0)PC	0.32 ± 0.02	2.19 ± 0.16
di(Br_2C18:0)PS	0.31 ± 0.02	2.88 ± 0.24
di(Br_2C18:0)PA	0.24 ± 0.02	2.76 ± 0.21
tetra(Br_2C18:0)CL	0.28 ± 0.02	1.34 ± 0.09
	F80W:K100Q	
di(Br_2C18:0)PC	0.25 ± 0.01	2.33 ± 0.06
di(Br_2C18:0)PS	0.24 ± 0.01	2.96 ± 0.15
di(Br_2C18:0)PA	0.16 ± 0.02	2.84 ± 0.24
tetra(Br_2C18:0)CL	0.20 ± 0.03	1.32 ± 0.11
	F80W:R98Q:K99Q:K100Q	
di(Br_2C18:0)PC	0.27 ± 0.02	2.33 ± 0.20
di(Br_2C18:0)PS	0.25 ± 0.02	2.29 ± 0.16
di(Br_2C18:0)PA	0.13 ± 0.01	3.12 ± 0.19
tetra(Br_2C18:0)CL	0.24 ± 0.02	1.23 ± 0.07
	F80W:V21K	
di(Br_2C18:0)PC	0.52 ± 0.01	2.15 ± 0.21
di(Br_2C18:0)PA	0.42 ± 0.01	2.88 ± 0.13

[a] F_0 and F are fluorescence intensities for MscL reconstituted in nonbrominated phospholipid and the corresponding brominated phospholipid, respectively, measured at pH 7.2. The value of *n* is the value obtained by fitting the data for the charged mutants of F80W reconstituted into mixtures of brominated lipid with the corresponding nonbrominated lipid to eq 1; the experimental data for F80W:R98Q:K99Q:K100Q are shown in Figure 3, and those for F80W:V21K are shown in Figure 5. [b] The number of lipid binding sites from which the fluorescence of the Trp residue can be quenched.

Table 3: Relative Lipid Binding Constants for Charge Mutants of MscL[a]

	relative binding constant	
phospholipid	measd using di(Br_2C18:0)PC	measd using di(C18:1)PC
	F80W	
di(C18:1)PS	1.66 ± 0.16	1.69 ± 0.10
di(C18:1)PA	1.81 ± 0.21	3.49 ± 0.25
	F80W:R98Q	
di(C18:1)PS	1.90 ± 0.26	1.20 ± 0.18
di(C18:1)PA	1.16 ± 0.26	1.69 ± 0.28
	F80W:K99Q	
di(C18:1)PS	1.06 ± 0.06	1.00 ± 0.09
di(C18:1)PA	1.10 ± 0.09	1.38 ± 0.19
	F80W:K100Q	
di(C18:1)PS	1.35 ± 0.12	1.06 ± 0.16
di(C18:1)PA	1.25 ± 0.22	1.51 ± 0.21
	F80W:R98Q:K99Q:K100Q	
di(C18:1)PS	1.30 ± 0.10	0.91 ± 0.10
di(C18:1)PA	1.08 ± 0.08	1.07 ± 0.05
	F80W:V21K	
di(C18:1)PA	1.30 ± 0.12	1.24 ± 0.16

[a] Binding constants relative to di(C18:1)PC were obtained by fitting the quenching data for charge mutants of F80W in mixtures of di(Br_2C18:0)PC with nonbrominated lipid or di(C18:1)PC with brominated lipid, as shown in Figure 4 for F80W:R98Q and F80W:R98Q:K99Q:K100Q and in Figure 5 for F80W:V21K, to eq 3, using the values for *n* given in Table 2.

one with a higher relative binding constant for phosphatidic acid than the other. Mutation of Arg-98, Lys-99, or Lys-100 results in a ca. 50% decrease in affinity for phosphatidic acid, with only a slightly higher affinity measured with di(Br_2C18:0)PA than with di(Br_2C18:0)PC (Figure 4; Table 3). Simultaneous mutation of all three charged residues results in a reduction of the relative binding constant for phosphatidic acid to a value close to 1, showing a total loss of selectivity for phosphatidic acid (Figure 4; Table 3). Selectivity of F80W for phosphatidylserine is less than that for phosphatidic acid, but again mutation of charged residues, particularly Lys-99 and Lys-100, results in a loss of specificity for phosphatidylserine (Figure 4, Table 3). It is possible that the loss of affinity for anionic lipids observed on mutation of the residues Arg-98, Lys-99, and Lys-100 follows from conformational changes on the protein rather than from the loss of the charges as such, particularly for the triple mutation that results in a gain of function phenotype. Figure 5 shows fluorescence quenching plots for F80W:V21K. The relative binding constants obtained for phosphatidic acid from the experiments with di(Br_2C18:0)-PC and with di(Br_2C18:0)PA are the same (Table 3), suggesting that in the gain of function mutant there is only a small selectivity for phosphatidic acid over phosphatidylcholine, the same at all sites.

Fluorescence quenching of L69W and Y87W. Leu-69 and Tyr-87 are located, respectively, at the periplasmic and cytoplasmic ends of the second transmembrane α-helix of MscL (Figure 1). Mutation of these resides to Trp did not result in either a gain of function or a loss of function phenotype (data not shown). Quenching of the Trp fluorescence of L69W by brominated phospholipids will report on lipid binding on the periplasmic side of the bilayer, and quenching of Y87W will report on lipid binding on the cytoplasmic side of the bilayer.

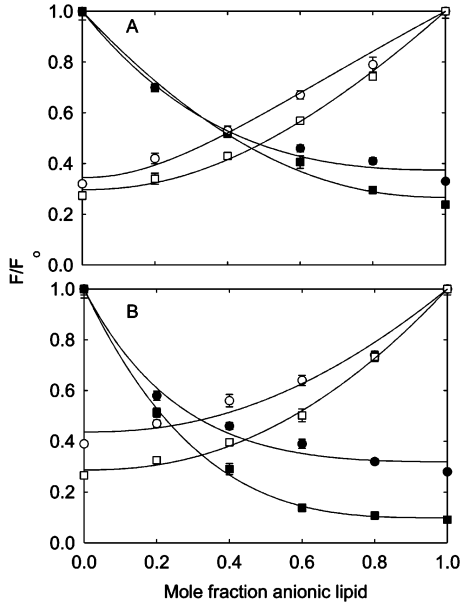

FIGURE 4: Quenching of Trp fluorescence of charge mutants of F80W in mixtures of anionic lipid and phosphatidylcholine. F80W:R98Q (●, ○) and F80W:R98Q:K99Q:K100Q (■, □) were reconstituted into mixtures containing di(C18:1)PC and brominated anionic phospholipid (filled symbols), or nonbrominated anionic phospholipid and di(Br_2C18:0)PC (open symbols). Anionic lipids: (A) phosphatidylserine; (B) phosphatidic acid. Fluorescence intensities are expressed as a fraction of the fluorescence for MscL reconstituted in mixtures of nonbrominated lipid. Data points are the average of three determinations. The solid lines show best fits to eq 3 giving the relative binding constants listed in Table 3.

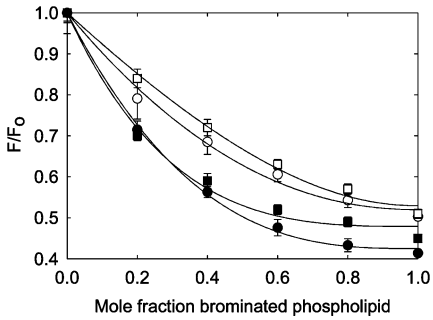

FIGURE 5: Quenching of the Trp fluorescence of F80W:V21K by brominated phospholipids. F80W:V21K was reconstituted into mixtures of (○) di(Br_2C18:0)PC and di(C18:1)PC, (□), di(Br_2C18:0)PC and di(C18:1)PA, (■) di(C18:1)PC and di(Br_2C18:0)PA, and (●) di(C18:1)PA and di(Br_2C18:0)PA. Fluorescence intensities are expressed as a fraction of the fluorescence for MscL reconstituted in mixtures of nonbrominated lipid. The solid lines show best fits to eqs 1 and 3 giving the values for *n* listed in Table 2 and the relative binding constants listed in Table 3.

Fluorescence quenching plots for L69W and Y87W reconstituted into mixtures of brominated lipid with the corresponding nonbrominated lipid fitted to eq 1 with the values for *n* given in Table 4. The values for *n* are similar to those for KcsA where the Trp residues are also located close to the ends of the transmembrane α-helices (*6*). Again, the value of *n* for cardiolipin is about half that for the other lipids, consistent with the four-chain structure of cardiolipin and the two-chain structure of the other lipids. The level of quenching observed for Y87W is greater than that observed with L69W (Table 4), consistent with a more peripheral location for position 69 than for position 87 (Figure 1). The level of quenching observed with anionic phospholipids is

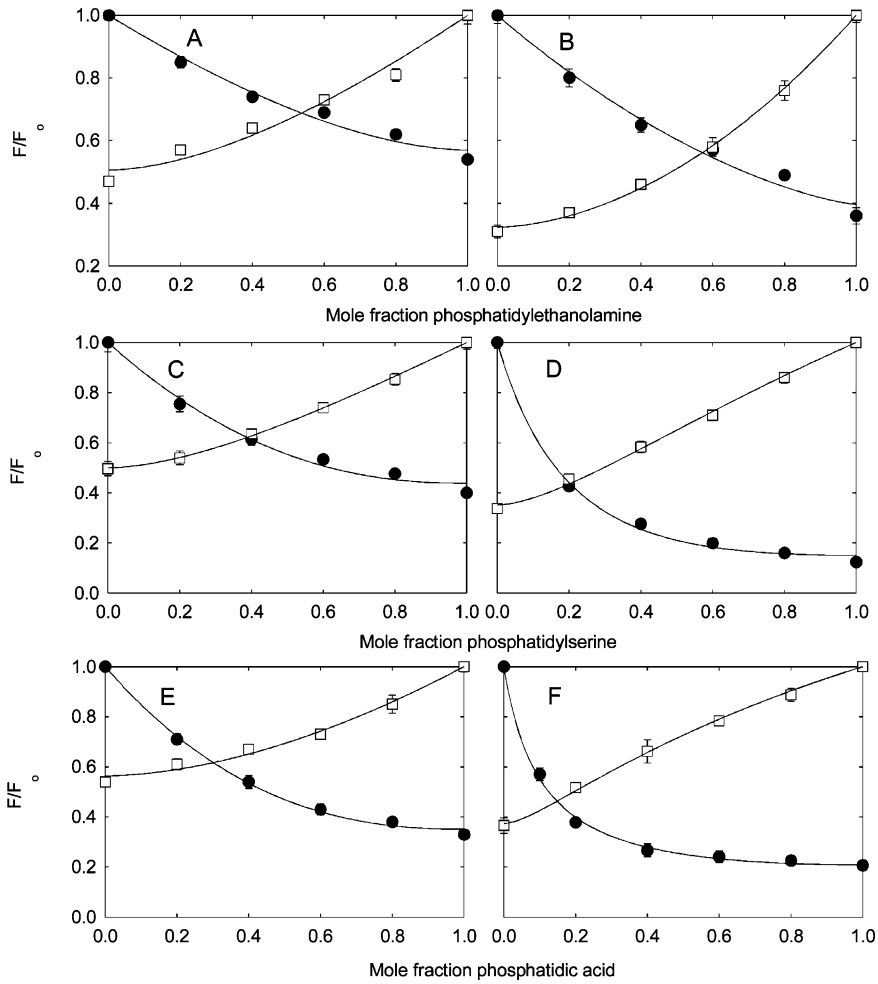

FIGURE 6: Quenching of Trp fluorescence of L69W and Y87W by brominated phospholipids. L69W (A, C, and E) and Y87W (B, D, and F) were reconstituted into bilayers containing mixtures of the following lipids: (A, B) (●) di(C18:1)PC and di(Br_2C18:0)PE and (□) di(C18:1)PE and di(Br_2C18:0)PC; (C, D) (●) di(C18:1)PC and di(Br_2C18:0)PS and (□) di(C18:1)PS and di(Br_2C18:0)PC; (E, F) (●) di-(C18:1)PC and di(Br_2C18:0)PA and (□) di(C18:1)PA and di(Br_2C18:0)PC. Fluorescence intensities are expressed as a fraction of the fluorescence for MscL reconstituted in mixtures of nonbrominated lipid. The solid lines show best fits to eq 3 giving the relative binding constants listed in Table 5.

Table 4: Fluorescence Quenching of L69W and Y87W in Brominated Phospholipids as a Function of Lipid Headgroup[a]

phospholipid	F/F_0	n[b]
	L69W (periplasmic)	
di(Br_2C18:0)PC	0.49 ± 0.01	1.79 ± 0.09
di(Br_2C18:0)PE	0.56 ± 0.02	1.80 ± 0.23
di(Br_2C18:0)PS	0.42 ± 0.01	2.29 ± 0.14
di(Br_2C18:0)PA	0.33 ± 0.01	2.26 ± 0.14
tetra(Br_2C18:0)CL	0.39 ± 0.02	1.10 ± 0.09
	Y87W (cytoplasmic)	
di(Br_2C18:0)PC	0.34 ± 0.01	1.75 ± 0.08
di(Br_2C18:0)PE	0.38 ± 0.02	1.35 ± 0.12
di(Br_2C18:0)PS	0.16 ± 0.01	1.93 ± 0.10
di(Br_2C18:0)PA	0.23 ± 0.02	2.05 ± 0.19
tetra(Br_2C18:0)CL	0.29 ± 0.01	1.01 ± 0.04

[a] F_0 and F are fluorescence intensities for MscL reconstituted in nonbrominated phospholipid and the corresponding brominated phospholipid respectively, measured at pH 7.2. The value of n is the value obtained by fitting the data for the charged mutants of F80W reconstituted into mixtures of brominated lipid with the corresponding nonbrominated lipid to eq 1. [b] The number of lipid binding sites from which the fluorescence of the Trp residue can be quenched.

again slightly greater than that observed with zwitterionic lipids (Table 4).

Table 5: Relative Lipid Binding Constants for MscL on the Periplasmic and Cytoplasmic Sides of the Membrane[a]

	relative binding constant	
phospholipid	measd using di(Br_2C18:0)PC	measd using di(C18:1)PC
	L69W (periplasmic)	
di(C18:1)PE	1.16 ± 0.24	0.90 ± 0.17
di(C18:1)PS	1.30 ± 0.06	1.00 ± 0.15
di(C18:1)PA	1.03 ± 0.14	1.12 ± 0.08
	Y87W (cytoplasmic)	
di(C18:1)PE	0.92 ± 0.05	1.21 ± 0.20
di(C18:1)PS	1.79 ± 0.13	2.96 ± 0.27
di(C18:1)PA	2.60 ± 0.20	4.42 ± 0.17

[a] Binding constants relative to di(C18:1)PC were obtained by fitting the quenching data for MscL mutants in mixtures of di(Br_2C18:0)PC with nonbrominated lipid or di(C18:1)PC with brominated lipid shown in Figure 6 to eq 3, using the values for n given in Table 4.

Figure 6A and Figure 6B show fluorescence quenching curves for L69W and Y87W in di(C18:1)PE/di(Br_2C18:0)-PC and di(Br_2C18:0)PE/di(C18:1)PC mixtures. The data fit to eq 3 with the binding constants for di(C18:1)PE relative to di(C18:1)PC given in Table 5. The fact that, within experimental error, the binding constants obtained from analysis of the di(C18:1)PE/di(Br_2C18:0)PC mixtures and

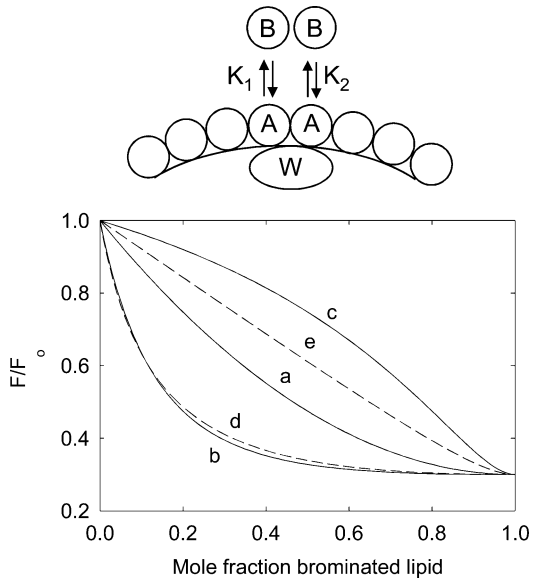

FIGURE 7: Simulations of fluorescence quenching in terms of the one set of sites and two sites models. Top: Binding of brominated lipid at the two sites shown results in quenching of the fluorescence of the Trp residue, described either in terms of a single set of identical binding sites with $n = 2$ (eq 3) or in terms of two sites with different affinities K_1 and K_2. Bottom: Simulations of F/F_0 in mixtures of brominated and nonbrominated lipids A and B: all simulations assumed a maximum fluorescence quenching of $F/F_0 = 0.3$ in brominated lipid. Curves a−c correspond to the single site model (eq 3) with $n = 2$. For curve a, the two lipids A and B bind with equal affinity ($K = 1$). For curves b and c the binding constant for B is four times that for A ($K = 4$); curve b corresponds to mixtures of nonbrominated A and brominated B, and curve c corresponds to mixtures of brominated A and nonbrominated B. Curves d and e (broken lines) correspond to the two site model (eq 5) with a binding constant for B at site 1 eight times that for A ($K_1 = 8$) with A and B binding with equal affinity at site 2 ($K_2 = 1.0$); curve d corresponds to mixtures of nonbrominated A and brominated B, and curve e corresponds to mixtures of brominated A and nonbrominated B.

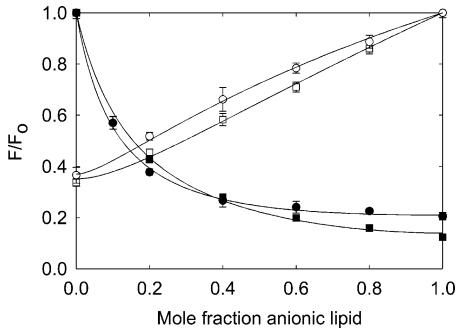

FIGURE 8: Quenching of Trp fluorescence of Y87W in mixtures of phosphatidylcholine and phosphatidylserine or phosphatidic acid. Y87W was reconstituted into mixtures containing di(C18:1)PC and di(Br_2C18:0)PS (■) or di(Br_2C18:0)PA (●), or into mixtures containing di(Br_2C18:0)PC and di(C18:1)PS (□) or di(C18:1)PA (○). The solid lines show best fits to eq 5 giving the relative binding constants listed in Table 6.

Table 6: Relative Lipid Binding Constants on the Cytoplasmic Side of the Membrane[a]

lipid	relative lipid binding constant	
	site 1	site 2
di(C18:1)PS	1.23 ±0.11	5.02 ± 0.61
di(C18:1)PA	1.69 ± 0.14	8.41 ± 0.54

[a] Binding constants relative to di(C18:1)PC were obtained by fitting the quenching data shown in Figure 8 for Y87W in mixtures of di(Br_2C18:0)PC with nonbrominated lipid or di(C18:1)PC with brominated lipid to eq 5 using the values for n given in Table 4.

of the di(Br_2C18:0)PE/di(C18:1)PC mixtures are the same confirms simple competitive binding of phosphatidylcholines and phosphatidylethanolamines to the lipid binding sites on MscL. Further, the observation that the values of the relative binding constants obtained with L69W and Y87W are both very close to 1 shows that there is no selectivity in binding zwitterionic lipids, on either side of the membrane.

A similar analysis was carried out for binding of anionic lipids (Figure 6C−F). For L69W, relative binding constants for the anionic lipids phosphatidylserine and phosphatidic acid were close to 1 and equal in the experiments with brominated phosphatidylcholine and with brominated anionic lipid, again showing simple competitive binding of phosphatidylserine or phosphatidic acid with phosphatidylcholine on the periplasmic side of the membrane. A very different pattern of results was obtained for quenching of Y87W in mixtures with anionic lipid. In this case the relative binding constants obtained for phosphatidylserine and phosphatidic acid were significantly different from 1, and the values obtained from experiments with the brominated anionic lipid were markedly higher than those obtained with brominated phosphatidylcholine (Figure 6D,F; Table 5). This suggests that, on the cytoplasmic side of the membrane, rather than simple competitive binding of lipids at a single class of site, there must be at least two classes of site with different affinities for anionic lipid.

Quenching by brominated anionic lipids on the cytoplasmic side of the membrane fits to a value of n close to 2, except for the four-chain brominated cardiolipin, where the value of n is 1 (Table 4). We have therefore assumed that there are two binding sites for the two-chain lipids sufficiently close to the Trp residue that binding of brominated lipid to these sites quenches the fluorescence of the Trp residue (Figure 7). We have then analyzed the data in terms of a two site model with equal quenching of Trp fluorescence from the two sites (eq 5), as illustrated in Figure 7. Relative association binding constants K_1 and K_2 at the two sites describe the affinity of the sites for lipid A relative to lipid B. When $K_1 = K_2$, eq 5 reduces to eq 3, the equation for a single set of lipid binding sites with $n = 2$. Figure 7 compares simulated fluorescence quenching curves for the single set of sites and two site models, all calculated assuming a maximum fluorescence quenching F/F_0 of 0.3. Curves a, b, and c correspond to the single set of sites model with $n = 2$, described by eq 3. Curve a shows a simulation for the case where lipids A and B bind equally well to the protein ($K = 1$). Curves b and c show simulations assuming that lipid B binds with an affinity four times that of A ($K = 4$), where curve b corresponds to mixtures of nonbrominated A and brominated B, and curve c corresponds to mixtures of brominated A and nonbrominated B. The observed much greater quenching observed at intermediate concentrations of brominated lipid in mixtures of nonbrominated A and brominated B (curve b) compared to that observed in mixtures of brominated A and nonbrominated B (curve c) follows simply from the stronger binding of lipid B to the protein. Curves d and e correspond to the two site model,

described by eq 5, assuming that lipid B binds with an affinity eight times that of A at site 1 ($K_1 = 8$) but binds with an affinity the same as that of A at site 2 ($K_2 = 1$). As shown by curve d, which corresponds to mixtures of nonbrominated A and brominated B, the fluorescence quenching curve obtained from the two site model with $K_1 = 8$ and $K_2 = 1$ is very similar to that obtained for the single set of sites model with $K = 4$. However, the quenching curve obtained from the two site model for mixtures of brominated A and nonbrominated B (curve e) is very different from the corresponding curve for the single site model (curve c); in particular, the greater level of quenching observed at intermediate levels of brominated A in curve e compared to curve c follows from the stronger binding of brominated A to site 2 in the two site model than to either site in the single set of sites model. As shown in Figure 8, the experimental data for quenching of Y87W in mixtures with anionic lipid fit well to the two site model with values for the relative binding constants at the two sites given in Table 6.

DISCUSSION

MscL opens when the tension in the surrounding membrane increases, and, because MscL is fully functional when reconstituted alone into lipid vesicles, membrane tension must be transduced directly from the lipid molecules to the protein (*15*, *16*). The strength of the coupling between MscL and the surrounding lipid molecules is likely to be dependent on the headgroup structure of the lipid molecules. Hydrogen bonding interactions will be more important for interaction with phosphatidylethanolamines than with phosphatidylcholines, and charge interactions will be more important for interaction with anionic lipids than with zwitterionic lipids (*1*, *11*). The importance of the interaction with the lipid headgroups is shown by the fact that loss of function mutants in MscL are concentrated on either side of the transmembrane domain, in regions that will interact with the lipid headgroups (*17*). Although the zwitterionic lipid in *E. coli* and *M. tuberculosis* is phosphatidylethanolamine (PE), most functional studies of MscL have used phosphatidylcholine (PC) as the lipid. The native membranes also contain significant amounts of anionic lipid, phosphatidylglycerol, and cardiolipin in the case of *E. coli*, and phosphatidylinositolmannosides and cardiolipin in the case of *M. tuberculosis* (*23*, *24*). It is not known whether coupling to the zwitterionic lipids or to the anionic lipids is most important for function of MscL.

Molecular dynamic simulations of MscL in bilayers of phosphatidylethanolamine show extensive hydrogen bond formation between the phosphatidylethanolamine headgroup and MscL, interactions that are not present for MscL in bilayers of phosphatidylcholine (*25*, *26*). The simulations also suggest that whereas the structure of MscL in bilayers of phosphatidylethanolamine is the same as in the crystal, the structure of MscL in bilayer of phosphatidylcholine is significantly different (*26*). Arg-45 and Asp-68 in the periplasmic loop region and Tyr-94 and Glu-102 in the C-terminal region interact more favorably with phosphatidylethanolamine than with phosphatidylcholine, and a rearrangement of the C-terminal region of MscL in phosphatidylcholine in which the C-terminal region moves closer to the membrane gives a stronger interaction of Lys-99, Lys-100, Asp-108, and Glu-116 with phosphatidylcholine than with phosphatidylethanolamine (*26*). Lys-99 and Lys-100 are part of a highly conserved charged region (*27*), and deletion of this region from the *E. coli* protein leads to loss of function (*28*).

Traditional methods for measuring lipid binding constants for membrane proteins give only an average value for all the lipid molecules binding to the surface of a membrane protein. However, the existence of regions of strong charge close to the membrane surface, like that in the C-terminal region of MscL (Figure 1), means that lipid binding to the surface of a membrane protein could be heterogeneous, with hot spots where anionic lipids can bind with an affinity much greater than their average affinity for the protein. The existence of such hot spots can be detected using Trp fluorescence quenching if the membrane protein contains a single Trp residue, making use of the fact that a brominated phospholipid molecule has to bind very close to a Trp residue in order to quench its fluorescence.

Lipid Binding on the Two Faces of the Bilayer. By introducing Trp residues at positions 69 and 87 on the periplasmic and cytoplasmic sides of the membrane, respectively (Figure 1), we can measure lipid binding constants in the two halves of the bilayer. As far as we are aware, this is the first reported measurement of this type. As shown in Table 5, phosphatidylethanolamine and phosphatidylcholine bind with equal affinity, on both the periplasmic and cytoplasmic sides of the membrane. Thus the greater number of hydrogen bonding interactions between phosphatidylethanolamine and MscL observed in molecular dynamics simulations (*26*) does not result in a stronger binding than for phosphatidylcholine. On the periplasmic side of the membrane, molecular dynamics simulations show only very small differences in the lipid−residue interaction energies between phosphatidylcholines and phosphatidylethanolamines (*26*). On the cytoplasmic side of the membrane, the molecular dynamics simulations suggest much larger changes in the energies of individual residue interactions with phosphatidylcholines and phosphatidylethanolamines (*26*), but presumably gains and losses largely cancel, resulting in the observed lack of selectivity on the cytoplasmic side of the membrane (Table 5).

On the periplasmic side, the binding constant for anionic lipids relative to that for di(C18:1)PC is close to 1 (Table 5). This lack of selectivity for anionic lipids on the periplasmic side of the membrane is consistent with the distribution of charged residues in MscL on the periplasmic side. The only positively charged residues on the periplasmic side are Arg-45 and Arg-58, on the top surface of the protein, pointing away from the lipid headgroup region. In contrast, the cytoplasmic side of the membrane shows a marked selectivity for anionic lipid (Table 5). In a previous study, based on fluorescence quenching studies with the F80W mutant of *M. tuberculosis* MscL reconstituted into bilayers containing phosphatidic acid, we determined a higher binding constant for phosphatidic acid from experiments with di(Br_2C18:0)PA than from experiments with di(Br_2C18:0)PC, suggesting the presence of a site on MscL with a high affinity for phosphatidic acid (*5*). Similarly, a higher binding constant is obtained from analysis of quenching data for Y87W with di(Br_2C18:0)PA or di(Br_2C18:0)PS than with di(Br_2C18:0)-PC (Table 5). In this case, an analysis is possible in terms of a two site model in which binding of brominated lipid to

either of two sites close to the Trp residue at position 87 causes fluorescence quenching, the two sites having different relative affinities for anionic lipid (Figure 7). The data fit well to this model (Figure 8) giving the binding constants listed in Table 6. Binding at one of the two sites shows a marked preference for anionic lipid, whereas binding at the other site shows only a slight preference for anionic lipid over phosphatidylcholine (Table 6). The number of lipid molecules required to form a complete bilayer shell around the MscL pentamer is ca. 29, since the circumference of MscL is ca. 135 Å and the diameter of a lipid molecule is ca. 9.4 Å. Thus the total number of lipid molecules in contact with each MscL monomer on the cytoplasmic side of the membrane is ca. 3. Given the distribution of charged residues on the cytoplasmic side of the protein, it is likely that the only site of high affinity for anionic lipids is that detected in the fluorescence quenching experiments.

Importance of Arg-98, Lys-99, and Lys-100 in Binding Anionic Lipids. On the cytoplasmic side of the membrane, the only positively charged residues in a position to interact with an anionic phospholipid headgroup are Arg-98, Lys-99, and Lys-100. To determine if this cluster of charged residues constitutes the hot spot for binding anionic lipid, we mutated these residues individually to Gln. As shown in Table 3, this resulted in a reduced affinity for phosphatidic acid, with smaller differences between the experiments with di(Br_2C18:0)PA and those with di(Br_2C18:0)PC. However, we also noted that single mutations of Arg-98, Lys-99, or Lys-100 in F80W resulted in a significant shift in the Trp fluorescence emission spectrum to longer wavelength in bilayers of di(C18:1)PC, consistent with a conformational change for the protein resulting in a shift of the Trp residue to a more polar environment (Table 1). However, we observed that the shift in Trp fluorescence emission observed in di(C18:1)PC for the single charge mutants was reversed when the mutated protein was reconstituted into bilayers of di(C18:1)PA or di(C18:1)PS (Table 1), suggesting that the conformational change induced by mutation of one of the three charged residues is reversed by binding of anionic lipid. This could be the reason why the single charge mutations did not result in a gain of function phenotype (Figure 2), the ca. 30 mol % anionic lipid present in the *E. coli* cell membrane (*24*) being sufficient to reverse the effect of the mutation on MscL. Single mutations of Arg-104, Lys-105, or Lys-106 in *E. coli*, equivalent to Arg-98, Lys-99, and Lys-100 in *M. tuberculosis* MscL, also resulted in no effect on growth rate (*17*). Given that the conformational effects of single charge mutations can be reversed by the presence of anionic lipid, the reductions in affinity for phosphatidic acid observed on mutation of Arg-98, Lys-99, or Lys-100 (Table 3) are consistent with the suggestion that these residues make up the headgroup binding region in the high affinity binding site for anionic lipid on MscL.

Effects of Simultaneous Mutation of Arg-98, Lys-99, and Lys-100. In contrast to the results with the single charge mutants, simultaneous mutation of Arg-98, Lys-99, and Lys-100 results in a larger shift of Trp fluorescence emission in di(C18:1)PC (Table 1) and the generation of a gain of function phenotype (Figure 2). Simultaneous mutation of all three charged residues also led to complete loss of selectivity for phosphatidic acid (Table 3). Experiments with V21K suggest that the conformational change resulting in the gain of function phenotype is, in itself, sufficient to cause loss of the high affinity binding site for phosphatidic acid. Mutation of Gly-22 in *E. coli* to a charged residue results in a gain of function mutation that restricts the rate of growth, with a channel that opens at very low tension and frequently occupies a subconductance state (*18*). Gly-22 in *E. coli* is equivalent to Val-21 in *M. tuberculosis*, and the mutation V21K results in a gain of function phenotype for *M. tuberculosis* MscL (Figure 2). The V21K mutation also results in a shift in Trp fluorescence emission in di(C18:1)-PC to longer wavelength, a shift that is not reversed in di-(C18:1)PA (Table 1). As shown in Table 3, F80W:V21K shows only a slight preference for phosphatidic acid over phosphatidylcholine, and the same values for the relative binding constant are obtained from experiments with di(Br_2-C18:0)PC and di(Br_2C18:0)PA. Since the three charged residues Arg-98, Lys-99, and Lys-100 are still present in F80W:V21K, this would suggest that the conformational change resulting in the gain of function phenotype is such as to break up the charge cluster, resulting in loss of the high affinity binding site for phosphatidic acid.

ACKNOWLEDGMENT

We thank Professor Rees for the generous gift of the wild-type MscL construct and Professor Booth for the generous gift of MJF465. We thank Dr. Jon Cooper for help with molecular modeling.

REFERENCES

1. Lee, A. G. (2003) Lipid-protein interactions in biological membranes: a structural perspective, *Biochim. Biophys. Acta 1612*, 1−40.
2. Marsh, D., and Horvath, L. I. (1998) Structure, dynamics and composition of the lipid-protein interface. Perspectives from spin-labelling, *Biochim. Biophys. Acta 1376*, 267−296.
3. East, J. M., Melville, D., and Lee, A. G. (1985) Exchange rates and numbers of annular lipids for the calcium and magnesium ion dependent adenosinetriphosphatase, *Biochemistry 24*, 2615−2623.
4. Davoust, J., and Devaux, P. F. (1982) Simulations of electron-spin resonance spectra of spin-labeled fatty acids covalently attached to the boundary of an intinsic membrane protein−a chemical exchange model, *J. Magn. Reson. 48*, 475−494.
5. Powl, A. M., East, J. M., and Lee, A. G. (2003) Lipid−protein interactions studied by introduction of a tryptophan residue: the mechanosensitive channel MscL, *Biochemistry 42*, 14306−14317.
6. Alvis, S. J., Williamson, I. M., East, J. M., and Lee, A. G. (2003) Interactions of anionic phospholipids and phosphatidylethanolamines with the potassium channel KcsA, *Biophys. J. 85*, 1−11.
7. Simmonds, A. C., East, J. M., Jones, O. T., Rooney, E. K., McWhirter, J., and Lee, A. G. (1982) Annular and non-annular binding sites on the (Ca^{2+} + Mg^{2+})-ATPase, *Biochim. Biophys. Acta 693*, 398−406.
8. Belrhali, H., Nollert, P., Royant, A., Menzel, C., Rosenbusch, J. P., Landau, E. M., and Pebay-Peyroula, E. (1999) Protein, lipid and water organization in bacteriorhodopsin crystals: a molecular view of the purple membrane at 1.9 Å resolution, *Structure 7*, 909−917.
9. Yankovskaya, V., Horsefield, R., Tornroth, S., Luna-Chavez, C., Miyoshi, C., Byrne, B., Cecchini, G., and Iwata, S. (2003) Architecture of succinate dehydrogenase and reactive oxygen generation, *Science 299*, 700−704.
10. Pebay-Peyroula, E., Dahout-Gonzalez, C., Kahn, R., Trezeguet, V., Lauquin, G. J. M., and Brandolin, G. (2003) Structure of mitochondrial ADP/ATP carrier in complex with carboxyatractyloside, *Nature 426*, 39−44.
11. Lee, A. G. (2004) How lipids affect the activities of integral membrane proteins, *Biochim. Biophys. Acta 1666*, 62−87.

12. East, J. M., and Lee, A. G. (1982) Lipid selectivity of the calcium and magnesium ion dependent adenosinetriphosphatase, studied with fluorescence quenching by a brominated phospholipid, *Biochemistry 21*, 4144−4151.
13. Bolen, E. J., and Holloway, P. W. (1990) Quenching of tryptophan fluorescence by brominated phospholipid, *Biochemistry 29*, 9638−9643.
14. Chang, G., Spencer, R. H., Lee, A. T., Barclay, M. T., and Rees, D. C. (1998) Structure of the MscL homolog from Mycobacterium tuberculosis: A gated mechanosensitive ion channel, *Science 282*, 2220−2226.
15. Sukharev, S. I., Sigurdson, W. J., Kung, C., and Sachs, F. (1999) Energetic and spatial parameters for gating of the bacterial large conductance mechanosensitive channel, MscL, *J. Gen. Physiol. 113*, 525−539.
16. Hamill, O. P., and Martinac, B. (2001) Molecular basis of mechanotransduction in living cells, *Physiol. Rev. 81*, 685−740.
17. Maurer, J. A., and Dougherty, D. A. (2003) Generation and evaluation of a large mutational library from the *Escherichia coli* mechanosensitive channel of large conductance, MscL—Implications for channel gating and evolutionary design, *J. Biol. Chem 278*, 21076−21082.
18. Yoshimura, K., Batiza, A., Schroeder, M., Blount, P., and Kung, C. (1999) Hydrophilicity of a single residue within MscL correlates with increased channel mechanosensitivity, *Biophys. J. 77*, 1960−1972.
19. Yoshimura, K., Nomura, T., and Sokabe, M. (2004) Loss-of-function mutations at the rim of the funnel of mechanosensitive channel MscL, *Biophys. J. 86*, 2113-2120.
20. Levina, N., Totemeyer, S., Stokes, N. R., Louis, P., Jones, M. A., and Booth, I. R. (1999) Protection of *Escherichia coli* cells against extreme turgor by activation of MscS and MscL mechanosensitive channels: identification of genes required for MscS activity, *EMBO J. 18*, 1730−1737.
21. London, E., and Feigenson, G. W. (1981) Fluorescence quenching in model membranes. 2. Determination of local lipid environment of the calcium adenosinetriphosphatase from sarcoplasmic reticulum, *Biochemistry 20*, 1939−1948.
22. O'Keeffe, A. H., East, J. M., and Lee, A. G. (2000) Selectivity in lipid binding to the bacterial outer membrane protein OmpF, *Biophys. J. 79*, 2066−2074.
23. Coren, M. B. (1984) Biosynthesis and structures of phospholipids and sulfatides, in *The Mycobacteria* (Kubica, G. P., and Wayne, L. G., Eds.) pp 379−415, Marcel Dekker, New York.
24. Harwood, J. L., Russell, N. J. Harwood, J. L., and Russell, N. J. (1984) *Lipids in Plants and Microbes*, George Allen & Unwin, London.
25. Elmore, D. E., and Dougherty, D. A. (2001) Molecular dynamics simulations of wild-type and mutant forms of the *Mycobacterium tuberculosis* MscL channel, *Biophys. J. 81*, 1345−1359.
26. Elmore, D. E., and Dougherty, D. A. (2003) Investigating lipid composition effects on the mechanosensitive channel of large conductance (MscL) using molecular dynamics simulations, *Biophys. J. 85*, 1512−1524.
27. Maurer, J. A., Elmore, D. E., Lester, H. A., and Dougherty, D. A. (2000) Comparing and contrasting *Escherichia coli* and *Mycobacterium tuberculosis* mechanosensitive channels (MscL)—New gain of function mutations in the loop region, *J. Biol. Chem. 275*, 22238−22244.
28. Blount, P., Sukharev, S. I., Schroeder, M. J., Nagle, S. K., and Kung, C. (1996) Single residue substitutions that change the gating properties of a mechanosensitive channel in *Escherichia coli*, *Proc. Natl. Acad. Sci. U.S.A. 93*, 11652−11657.
29. Rooney, E. K., and Lee, A. G. (1986) Fitting fluorescence emission spectra of probes bound to biological membranes, *J. Biochem. Biophys. Methods 120*, 175−189.
30. Esnouf, R. M. (1999) Further additions to MolScript version 1.4, including reading and contouring of electron-density maps, *Acta Crystallogr., Sect. D 55*, 938−940.
31. Powl, A. M., Wright, J. N., East, J. M., and Lee, A. G. (2005) Identification of the hydrophobic thickness of a membrane protein using fluorescence spectroscopy: studies with the mechanosensitive channel MscL, *Biochemistry*, in press.

BI047439E